Review of Silicon Carbide Power Devices and Their Applications

Xu She, *Senior Member, IEEE*, Alex Q. Huang, *Fellow Member, IEEE*, Óscar Lucía, *Senior Member, IEEE*, and Burak Ozpineci, *Senior Member, IEEE*

***Abstract*—Silicon carbide (SiC) power devices have been investigated extensively in the past two decades, and there are many devices commercially available now. Owing to the intrinsic material advantages of SiC over silicon (Si), SiC power devices can operate at higher voltage, higher switching frequency, and higher temperature. This paper reviews the technology progress of SiC power devices and their emerging applications. The design challenges and future trends are summarized at the end of the paper.**

***Index Terms*—Power converter, power device, review, silicon carbide (SiC).**

I. Introduction

THE evolution of power electronics technology has always moved toward higher efficiency, higher power density, and more integrated systems [1], [2]. Power semiconductor devices play a critical role in this nonstop evolution. To date, the advancements have been primarily driven by various Si power devices developed and matured over the last 50 years. In applications below 600 V, Si metal−oxide−semiconductor field-effect transistors (MOSFETs) based on trench gate structure dominate the market, whereas Si super junction MOSFETs and Si-insulated gate bipolar transistors (IGBTs) based on field stop and injection enhancement concepts dominate the market from 600 to 6.5 kV. Despite these advancements, Si power devices are approaching their performance limitations. The maximum blocking voltage of the IGBT is lower than 6.5 kV, and the practical operating temperature is lower than 175 °C [3]. Because of the bipolar current conduction mechanism in IGBTs, their switching speeds are also relatively slow, limiting them to lower switching-frequency applications. Future development in Si power device technologies will continue, but it will be incremental in nature. A revolutionary development in recent entry years has been the introduction of power devices based on wide bandgap (WBG) materials such as silicon carbide (SiC). As a WBG material, SiC has several superior material properties that are attractive for power device design; these are summarized in Fig. 1 in comparison with Si [3]–[5].

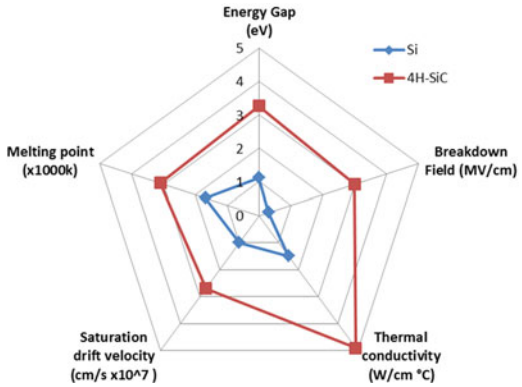

Fig. 1. Material properties comparison between Si and SiC (ranges 1−5 are marked for all five properties) [3].

Owing to the much wider energy bandgap of a 4H-SiC material compared with Si, its intrinsic carrier density is much smaller, which enables a high-temperature operation capability from a blocking stability point of view. The 10× critical electric field in SiC makes ultra–high-voltage (>10 kV) power devices practically achievable. The ideal specific conduction resistance ($R_{\mathrm{on,sp}}$) of a SiC unipolar device can be much smaller than that of its Si counterpart. The smaller $R_{\mathrm{on,sp}}$ enables SiC chips to be smaller, leading to lower parasitic capacitance and higher switching speed. Therefore, it is possible to achieve both low switching loss and low conduction loss for a wide range of blocking voltages and frequencies. The lower loss enables simpler power converter structures because simple two-level topologies can be used in most applications. So SiC power devices will enable further rapid evolution of power electronics systems toward even higher efficiency and power density. Although SiC dies can operate at higher temperatures, the peripheral components—such as the package materials, housings, and capacitors—are not yet mature. Therefore, the exploration of these components lags behind the progress in reaching higher voltages and higher frequencies.

Since the introduction of the first commercial SiC Schottky diode by Infineon in 2001, there has been a strong momentum

Manuscript received September 12, 2016; revised November 3, 2016; accepted December 4, 2016. Date of publication January 16, 2017; date of current version September 11, 2017.

X. She is with Electrical Power, GE Global Research, Niskayuna, NY 12309-1027 USA (e-mail: xshe@ieee.org).

A. Q. Huang is with North Carolina State University, Raleigh, NC 27696-7571 USA (e-mail: aqhuang@ncsu.edu).

Ó. Lucía is with Electronic Engineering and Communications, University of Zaragoza, 50018 Zaragoza, Spain (e-mail: olucia@ieee.org).

B. Ozpineci is with the Oak Ridge National Laboratory (ORNL), Knoxville, TN 37932 USA, and also with The University of Tennessee, Knoxville, TN 37996 USA (e-mail: burak@ornl.gov).

Color versions of one or more of the figures in this paper are available online at http://ieeexplore.ieee.org.

Digital Object Identifier 10.1109/TIE.2017.2652401

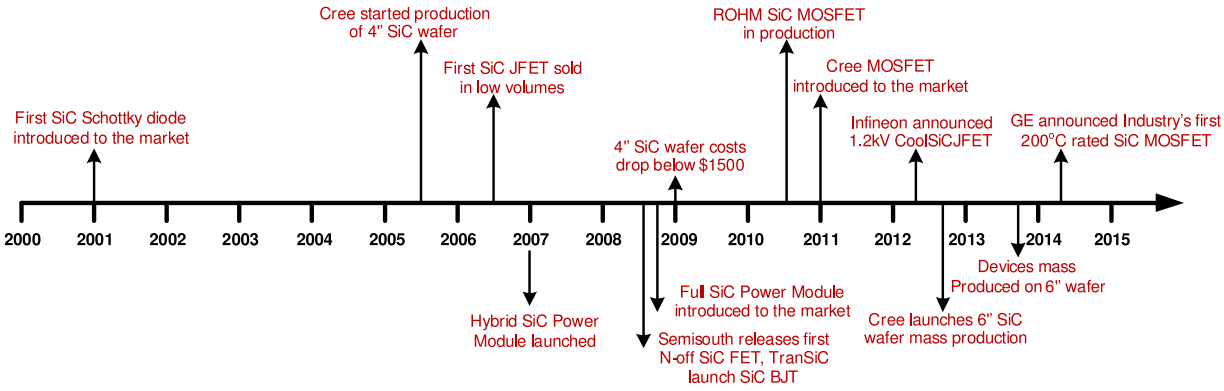

Fig. 2. SiC devices development milestones [6].

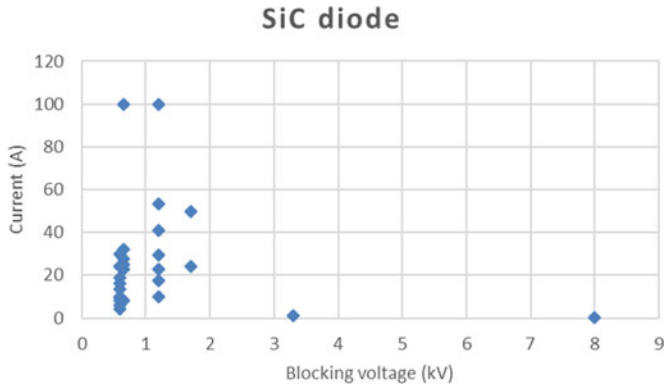

Fig. 3. Commercially available SiC discrete diode ratings @25 °C.

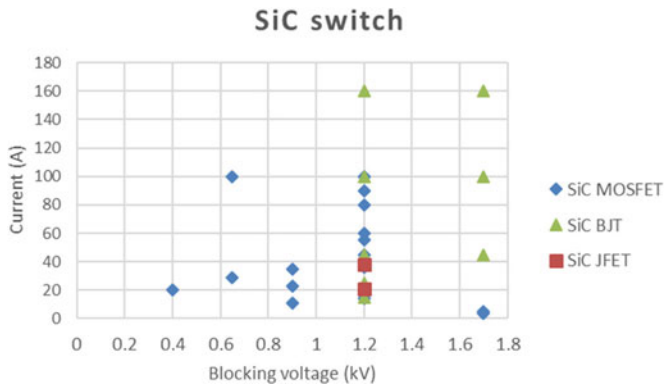

Fig. 4. Commercially available SiC discrete switch ratings @25 °C.

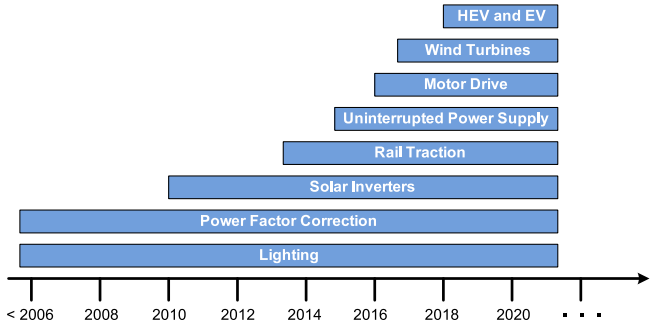

Fig. 5. SiC device application roadmap predicted by Yole [7].

in SiC technology development and market growth. Fig. 2 summarizes some key SiC development milestones [6]. Fig. 3 shows ratings of the discrete SiC diodes available from the major market players. Until now, the unipolar SiC diode is the only commercially available diode on the market; its typical voltage ratings are 600 V, 650 V, 1.2 kV, and 1.7 kV. These devices are significantly faster than Si PIN diodes because there is no minority carrier storage in the SiC diode. Some 3.3 and 8 kV products also are available, as shown in Fig. 3; however, their current rating is limited by the thick drift layer. For instance, the current rating for 8 kV SiC diode is only 50 mA. Fig. 4 shows the rating plot of SiC active switches available in the market in discrete packages. These include SiC MOSFETs, junction gate field-effect transistors (JFETs), and bipolar junction transistors (BJTs). Previously, the SiC JFET was more favorable because of its easy implementation and because it does not exhibit the gate-oxide reliability issue observed in the SiC MOSFET. Although its "normally on" characteristic makes it less attractive in some applications, a JFET with a cascode structure could eliminate this issue. The commercial SiC MOSFET was first released in 2011 by Cree. For the SiC MOSFET, the 1.2 kV class became the entry and dominant point in the market, as this is the breaking point between Si MOSFETs (including the super junction MOSFET) and the Si IGBT. The SiC MOSFET provides excellent balance between conduction loss and switching loss at blocking voltages of less than 2.5−3.3 kV. The SiC BJT's switching speed is similar to that of the MOSFET owing to the absence of any sizable minority carrier storage in the drift region. Since the BJT does not have a channel region, its on resistance is lower than that of the SiC MOSFET (see Fig. 4). However, the current driving characteristic makes it less attractive for various applications.

Fig. 5 shows the SiC device application roadmap predicted by Yole development [7]. SiC has found commercial applications in power factor correction, lighting, solar, railway traction, and uninterrupted power supply (UPS) and will enter into drive, wind, and electric vehicle (EV) applications soon. Aside from the technical design challenges, balancing the higher cost of SiC devices with improved system performance is the most critical issue. The cost per watt is one of the most concerning figures of merit from a user perspective. Depending on the application, a higher device cost does not necessary lead to a higher system

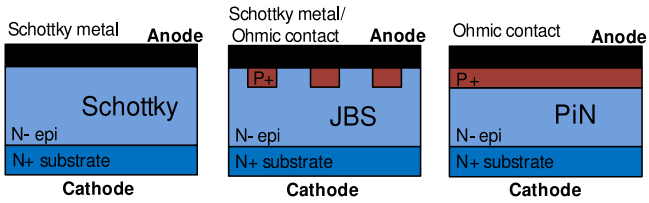

Fig. 6. Three basic SiC diode structures.

cost, and this will be explained in later section. As can be seen, SiC devices and power conversion systems have entered the commercialization stage. The major focuses of industry depend on the application demand, cost, and process maturity. From the technology development point of view, the potential of SiC materials is not fully explored and much more efforts are ongoing. The following sections of this paper review the technology advancements of SiC power devices and the critical applications and present the future challenges and development trends.

II. SiC Power Device Review

This section reviews the most promising commercial SiC power devices, including diode and MOSFET. Some other types of devices that have been commercialized, such as the SiC JFET and the BJT, also provide excellent performance; however, they are less attractive from industry application perspective. Therefore, they are not covered in this section. In addition, the state-of-the-art research developments in the high-voltage portfolio are reviewed, such as high-voltage IGBT, gate turn-off (GTO) thyristor, and emitter turn-off (ETO) thyristor.

A. SiC Diodes

There are three main types of SiC diodes: the SiC Schottky diode, the SiC junction barrier Schottky (JBS) diode, and the SiC PIN diode. The basic structures are shown in Fig. 6 [8].

Its combination of a Schottky diode structure and SiC material makes the SiC Schottky barrier diode (SBD) an ideal replacement for the Si PIN diode. In the forward state, current conduction is by the majority carrier electron current flowing from the anode to the cathode. The voltage drop is determined by the N-layer resistance plus that of the Schottky barrier height, which is typically 0.7–0.9 V. The device switches rapidly from ON to OFF, and there is virtually no reverse recovery current as result of the majority carrier conduction mechanism. The only current required to flow in the reverse direction is to charge the junction capacitance. This extremely fast reverse recovery characteristic is its most significant advantage over the Si PIN diode. In addition to enabling potential efficiency improvements, the low reverse recovery current also significantly reduces the converter oscillation and the related electromagnetic interference (EMI) problem during diode turn-off.

In the SBD, the leakage current at higher temperatures increases quickly as result of the Schottky barrier lowering effect; hence, the blocking voltage of commercially available SiC SBDs is limited to 600 V. Most of the commercialized SiC diodes shown in Fig. 3 use the JBS structure. In the SiC JBS diode, multiple P+ regions are integrated to surround the

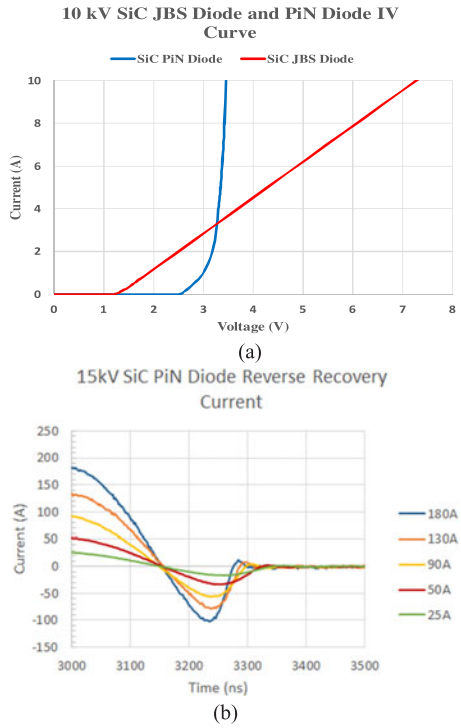

Fig. 7. (a) Ten-kilovolt SiC JBS diode and PIN diode $I-V$ curves at room temperature with the same chip size. (b) Reverse recovery current tested at $V_R = 7$ kV for a 15-kV SiC PIN diode ($T = 25$ °C).

Schottky region. They push the maximum electrical field away from the Schottky barrier toward the bottom of the P+ region. Therefore, the off-state leakage current is reduced even at the rated junction temperature, which is typically below 175 °C. Because the device conduction is still via majority carrier electrons, the speed of the JBS is not compromised. The JBS diode therefore provides excellent performance over a wide range of voltages, e.g., 600 V–3.3 kV. A 15-kV JBS diode has also been designed and tested for high-frequency applications [9]. However, the reliable voltage blocking capability still must be proved as the blocking voltage were shown to be around 13 kV in the tested samples. Another operating mode of this structure is called the merged PIN Schottky (MPS) diode; the internal PIN junction diode is turned on only under a large forward bias, thereby increasing the current handling capability. Progress has been made toward multiple generations of the SiC JBS/MPS diode in the power semiconductor industry [10]. Infineon has announced its fifth-generation SiC MPS diode produced in a thinner wafer. The thinner form provides a higher inrush current capability and lower thermal impedance. The trench structure SiC Schottky diode is also demonstrated to further reduce the leakage current [11]. A recent study also shows that modern SiC Schottky diodes have proved to be extremely robust against leakage current thermal runaway, as the required temperature rise for doubling the leakage current is higher than in the Si PIN diode [12].

The bipolar SiC PIN diode can effectively reduce the drift region resistance via conductivity modulation. This makes it promising in ultra–high-voltage ranges such as 10–20 kV [13]. In Fig. 7(a), the $I-V$ curves of a 10-kV SiC JBS diode and of a 10-kV PIN diode with same chip size are compared. Although it

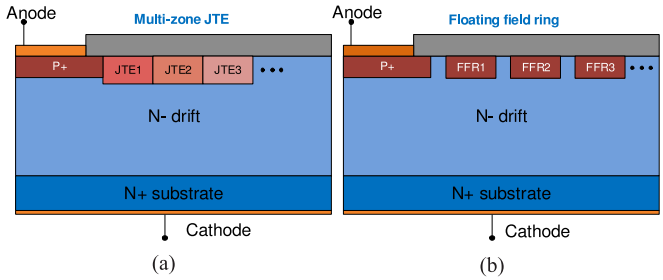

Fig. 8. Edge termination methods for high-voltage SiC devices. (a) Multizone JTE termination. (b) FFR termination.

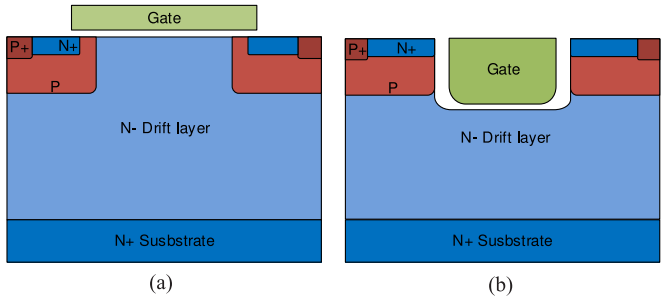

Fig. 9. Two typical SiC MOSFET structures: (a) planar and (b) trench.

has a higher knee voltage, the differential resistance of the SiC PIN diode is much smaller than that of the JBS diode owing to the conductivity modulation. Another advantage of the SiC PIN diode is its much lower leakage current compared with the JBS or SBD, making it an ideal candidate for higher temperature operation. However, the ∼3 V PN junction knee voltage, which is determined by the SiC material, makes the SiC PIN ineffective from the conduction point of view when the blocking voltages are below 3.3 kV. SiC JBS diodes are preferred in these voltage ranges. Because of the minority carrier stored in the device, there is also a sizeable reverse recovery current in the SiC PIN diode, as clearly shown in Fig. 7(b), resulting in large reverse recovery loss in converter applications.

For high-voltage SiC devices, one of the critical technical challenges that must be addressed is the surface electrical field reduction at the edge of the device. Numerous planar edge termination techniques have been demonstrated in SiC diodes, most of them based on similar concepts used in Si power devices. The most fundamental ones include junction termination extension (JTE) [14]–[16], floating field ring (FFR) [17]–[19], field plates [20], [21], mesa structure [22], bevel structure [23], [24], and hybrid solution methods [25]–[28]. The JTE and FFR are regarded as the most effective methods for high-voltage SiC devices [29]. The idea for the JTE is to extend the junction in the lateral direction and reduce the electric field crowding at the edge of the extension. Although a single-zone JTE conceptually works, it shows a narrow window of dose optimization range to achieve the desired voltage. As an improvement, Fig. 8(a) shows the case of a multiple-zone JTE concept, in which the dose is gradually decreased toward the JTE edge [15]. Doing so makes the shape of the electrical field distribution more rectangular instead of triangular, thereby increasing the breakdown voltage. The challenge for a multiple-zone JTE is the process complexity due to the multiple implant processes needed. Several single-implant multizone JTE methods are proposed that involve creating unsymmetrical shapes and/or distances among the zones [31]–[33]. In [31], the vertical depth of the JTE zone is gradually decreased toward the edge of the extension. In [32] and [33], the width of the zone, as well as the spacing, is controlled to smooth out the electrical field. Fig. 8(b) shows a cross-section diagram of the FFR termination method [17]–[19]. A single implant can be used for both the ring and the main junctions, thereby reducing the processing steps. However, the optimization of the spacing between the floating zones is complex and challenging.

B. SiC Switches

The most popular SiC switch is the MOSFET, as it nicely fits into the 1.2–3.3 kV blocking voltage requirement for many industrial applications. Compared with Si IGBTs, it significantly reduces the switching loss via its majority carrier conduction mechanism. Under certain conditions, zero switching loss can also be achieved, and operation at 3.38 MHz was recently demonstrated for a 1.2 kV SiC MOSFET module [34]. In addition, MOSFET can operate in the third quadrant as a synchronous rectifier, significantly reducing the third-quadrant conduction loss while offering almost zero reverse recovery losses. This also eliminates the need for an anti-parallel JBS diode. The body PIN diode conducts only during the dead time. One of the key challenges is to trade off the gate-oxide reliability for low specific on resistance. The previous gate−oxide stability issue has been solved and excellent reliability performance is achieved [35]. The industry's first reliable SiC MOSFET with a 200 °C junction temperature was also demonstrated by General Electric (GE) [36], [37]. There are two basic types of SiC MOSFET structures—the planar SiC MOSFET and the trench SiC MOSFET, as shown in Fig. 9 [38]. Fig. 9(a) shows a typical cross-section view of the planar SiC MOSFET structure. The on resistance of the SiC MOSFET has three main aspects—channel resistance, JFET region resistance, and drift region resistance [39]. For lower voltage devices (<1.2 kV), the substrate resistance is also substantial and cannot be ignored. A wafer-thinning technique can be used to reduce it. Another longstanding issue for the SiC MOSFET is its low channel mobility, which results in a higher percentage of resistance coming from this part of the device. Improving channel density can alleviate this problem. Fig. 9(b) shows the SiC trench MOSFET structure, which eliminates the JFET region and improves the channel density. Therefore, the specific on resistance can be reduced.

The first commercial trench MOSFET was released by Rohm in 2010. A novel double trench structure has been proposed to solve the oxide breakdown at the bottom of the trench [39]. Another consideration in applying SiC MOSFETs is the higher required gate voltage (18–20 V), which makes the traditional gate driver incompatible with the SiC MOSFET. This is especially challenging for some hybrid switch concepts [40], [41]. To solve this problem, Infineon has announced its newest SiC trench MOSFET with a 15/−5 V gate voltage and very low specific on resistance (3.5 $m\Omega \cdot cm^2$) [42].

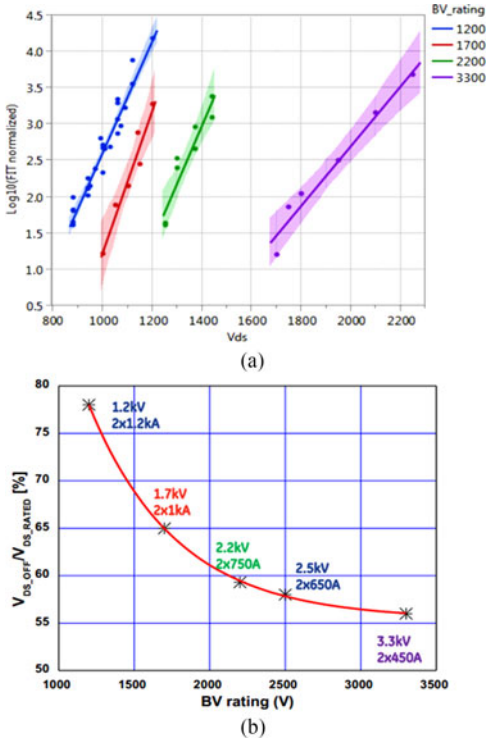

Fig. 10. SiC MOSFET with total active area of 7.2 cm^2, room temperature, and sea level [45]. (a) Failure caused by terrestrial cosmic radiation; (b) voltage derating guideline for failure rate of 100.

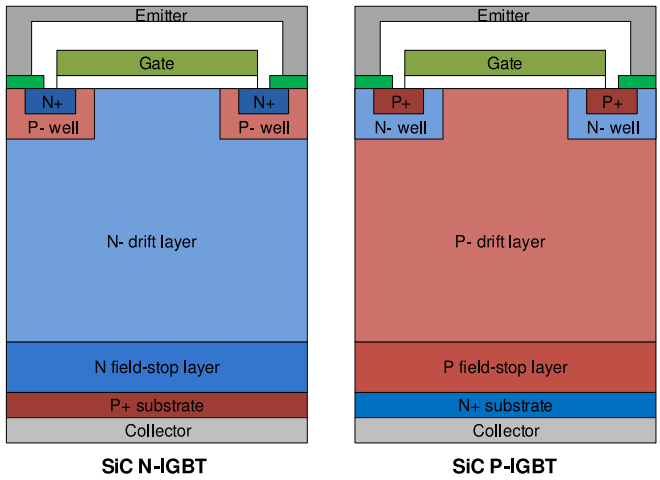

Fig. 11. Cross-section structure of SiC IGBT.

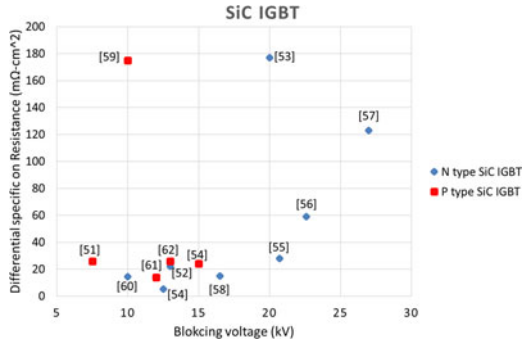

Fig. 12. Summary of high-voltage SiC IGBTs in the literature.

In addition to improved electrical performance, another major driver for SiC MOSFET innovation is reliability, one of the most critical concerns of end-users. High-temperature gate bias, high-temperature reverse bias, and high-humidity, high-temperature reverse bias are the three major criteria for evaluating reliability [43]. Highly reliable SiC devices have been successfully demonstrated in some commercialized products [35], [36], [44]. For instance, the reliability of the industry-leading 200 °C-rated SiC MOSFET was reported by GE in 2014 [36]. Another important parameter for power semiconductors is immunity to cosmic rays. This is especially important in applications such as aerospace and nuclear plant. In [45], 1.2–3.3 kV SiC MOSFETs with fewer than ten failures in time (FIT) were demonstrated, as shown in Fig. 10(a). This FIT rate is similar to that of the Si IGBT. The recommended derating curve is also provided as a guideline [see Fig. 10(b)]. A higher derating factor is needed for SiC devices with higher blocking voltages. Additional studies are needed to explain the physics behind this characteristic.

High-voltage SiC MOSFETs have also been reported to replace high-voltage Si devices from 3.3 to 6.5 kV and even higher voltages [46]–[49]. The highest blocking voltage reported for SiC MOSFET is 15 kV [47]. The high-voltage SiC MOSFET can simplify the circuit topology for high-voltage and high-frequency applications, such as solid-state transformers [50]. Although the high-voltage SiC MOSFET shows much reduced switching losses compared with the Si IGBT, the voltage drop becomes unacceptable, especially for voltage levels higher than 10 kV. In this condition, the combination of the SiC and bipolar device structure, such as SiC IGBT, would be desirable. Fig. 11 shows typical cross-section diagrams of N-type and P-type high-voltage SiC IGBTs. Normally, a buffer layer, or field-stop layer, is needed to prevent field punch-through and to achieve high injection efficiency from the substrate. Since electrons have 10× higher mobility than holes in 4H-SiC, the N-IGBT has a faster switching speed than the P-IGBT. However, the P-IGBT has several potential benefits, such as higher transconductance and easier manufacture of the N+ substrate.

Several high-voltage SiC IGBT designs have been reported [51]–[62]. Fig. 12 plots some of the reported SiC IGBTs with different blocking voltages and differential specific on resistance. The highest blocking voltage reported so far for an N-IGBT is 27 kV, obtained by using a 230 μm drift layer [57]. The design also incorporated a lifetime enhancement process to reduce the voltage drop. The highest blocking voltage reported for a P-IGBT is 15 kV, as shown in [54]. The differential specific on resistance for most of the reported SiC IGBTs is in the range of tens of milliohms.

The SiC GTO transistor has also been investigated. It achieves the best current-handling capability with a very low forward drop among all reported high-voltage SiC power devices, thanks to the double-side carrier injection and strong conductivity modulation [63]. This is clearly illustrated in Fig. 13, where the forward conduction characteristics of the 15 kV P-GTO, IGBT, and MOSFET are measured and compared. All these high-voltage devices are based on 4H-SiC material and fabricated by Cree. To

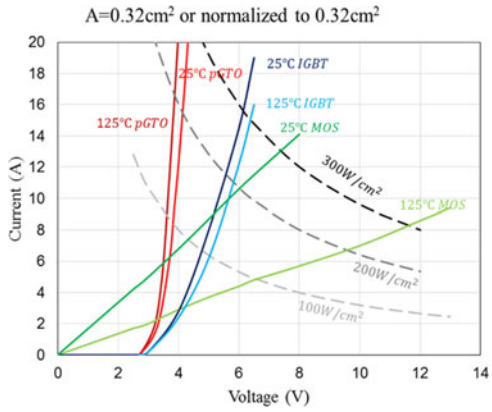

Fig. 13. *I–V* curve comparison of 15 kV SiC P-GTO, IGBT, and MOSFET at 25 °C and 125 °C.

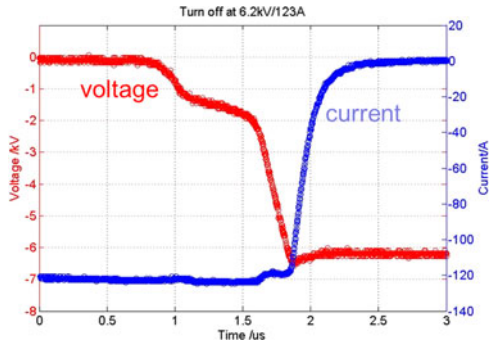

Fig. 14. Turn-off waveform of the 15 kV SiC P-ETO at 6.2 kV and 123 A.

minimize the effects of different chip sizes, the active chip areas are normalized to 0.32 cm^2 in Fig. 13. The SiC P-GTO shows the smallest voltage drop among all three types of devices, followed by the SiC IGBT and SiC MOSFET. In addition, instead of positive temperature coefficient shown in SiC MOSFET and IGBT, the SiC GTO transistor has a slight negative temperature coefficient of voltage drop. Based on SiC P-GTO technology, a 15-kV SiC ETO transistor has also been demonstrated [64]. Fig. 14 shows the turn-off waveform of the 15-kV SiC P-ETO. It is noted that the voltage and current are plotted in the negative region due to the P-type device. The peak power density reached 1.13 MW/cm^2, indicating a very large reverse bias safe operation area for SiC bipolar devices. This characteristic is very important for converter and circuit breaker applications.

III. SiC System Applications Review

As discussed earlier, SiC MOSFETs and JBS diodes provide superior dynamic performance compared with Si IGBTs and PIN diodes; therefore they can clearly improve power efficiency and power density. SiC MOSFET/IGBT/GTO/PIN devices also clearly have the capability to significantly expand the voltage range over the range available in Si power devices. Doing so will clearly increase the ability to develop new power electronics systems that were not practical before. However, widespread adoption of SiC power conversion systems is still challenging. One reason is that SiC is by no means a plug-and-play technology. Integrating SiC technology into the electrical system requires a deep understanding of system design, including EMI and thermal issues. Moreover, the relatively higher cost of SiC devices is a concern for end users. In fact, cost issues for SiC devices should be looked at from two aspects. First, the cost of SiC MOSFETs decreases with volume production [44]. With larger volumes, better manufacturing processes with larger wafers, and improved device performance, the cost per amp of SiC devices will drop. Second, it is known that the absolute cost of SiC devices is higher than the cost of Si devices because of intrinsic higher material costs. However, the per-watt cost of the overall system could potentially be reduced with a better balance-of-plant system design. Fig. 15 shows the potential system cost savings from using SiC power conversion systems. The savings may come from developments such as a smaller passive component, lower cooling requirements, and a higher absolute power rating. It is demonstrated in [65] that the cost of a 17 kW solar inverter could be reduced by 20% with SiC JFETs and SiC diodes. Additionally, the operational cost reduction gained from efficiency improvements could justify the higher capital cost, e.g., in UPS applications [66].

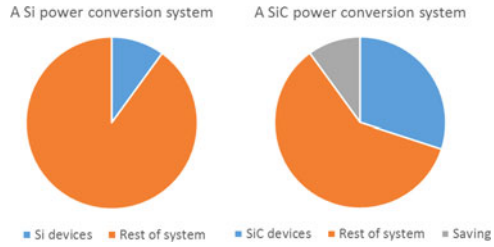

Fig. 15. Potential system cost benefit from SiC devices.

This section reviews some of the latest and representative developments of SiC devices in some critical and emerging industrial applications, such as solar, UPS, traction, EVs, and induction heating (IH).

A. SiC Solar Inverter

In the past decade, the solar inverter has progressed toward higher efficiency, higher density, and lower cost. SiC devices have been investigated in different types of solar inverters. In [67] and [68], SiC Schottky diode–based solar microinverters were demonstrated with reduced reverse recovery losses and improved efficiency. For rooftop applications, a desirable weight density is necessary, e.g., 1 kW/kg. Most commercialized products with Si IGBTs cannot fulfill this requirement; their weight density is less than 0.38 kW/kg. To address this challenge, Mookken *et al.* [69] present a 50-kW SiC MOSFET-based photovoltaic string inverter with significantly increased switching frequency and reduced weight, which achieves the design target. High-power centralized inverters based on SiC devices have also been developed. A 1 MW solar converter system consisting of a boost converter with an all-SiC power module and a Si-based three-level, T-type, neutral point–clamped structure is presented in [70]. The maximum achieved efficiency is 98.8% at 850 V, which is the upper maximum power point range limit. The total efficiency is about 0.5% higher than that of a traditional Si-based

Fig. 16. GE 1MW SiC inverter installed in Berlin.

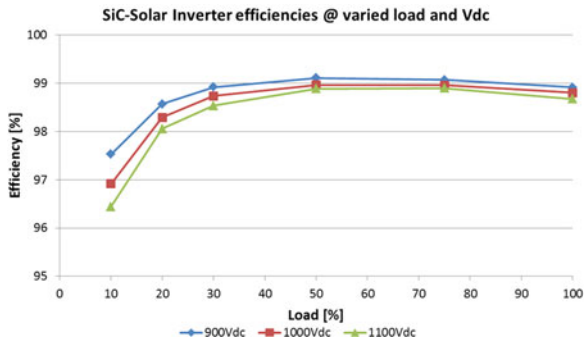

Fig. 17. Efficiency curve of GE SiC megawatt photovoltaic inverter [71].

single-stage-inverter. Recently, GE made another breakthrough with a full-SiC single-stage megawatt-level photovoltaic inverter (see Fig. 16) [71]. With an industry-leading SiC MOSFET module and innovative system engineering design, the reported California energy commission (CEC) efficiency is close to 99% at 900 V dc input (see Fig. 17).

B. Uninterrupted Power Supply

High efficiency, high power quality, and high power density are some of the main drivers for innovation in UPS systems, especially for the online double-conversion UPS. A UPS is located at the user (power purchaser) end. This means that the cost of electrical losses in the power conversion stage (e.g., the electricity bill) is two to three times higher than the capitalized loss cost at the generation end—a big advantage for highly efficient SiC converters. The higher efficiency means lower electric usage and cooling effort. In addition, the total cost of ownership is lower. The other factor that differentiates a UPS is that the system is typically housed in an office building, factory building, or data center, where floor space is at a premium and a compact, high-power-density system is highly desirable. For a 250 kVA UPS system using a Si-based three-level converter structure, 96% efficiency can be achieved at 50% load (the normal operating point) [66]. With SiC devices, a high-efficiency two-level solution becomes feasible [66], [72]–[74]. In [66],

TABLE I
COMPARISON OF SI AND SIC 500 kVA UPS FROM TOSHIBA

	Si UPS (G9000)	SiC UPS (G2020)
Dimensions (inch)	70.9 × 32.7 × 80.7	59.1 × 33.5 × 80.67
Weight (lb)	3360	2756
Efficiency	97%	98.2%

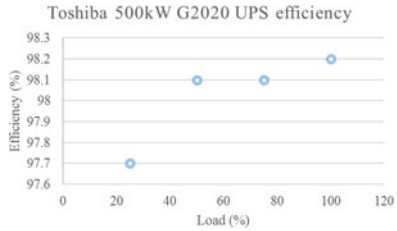

Fig. 18. Toshiba SiC 500 kW G2020 UPS efficiency curve [74].

it is shown that 97.6% efficiency could be obtained in a two-level SiC UPS with 32 kHz switching frequency, compared with 96% efficiency in a three-level Si UPS with 16 kHz switching frequency. Toshiba released its full-SiC UPS G2020 in 2015. The comparisons between the Si- and SiC-based UPS system, including size, weight, and efficiency, are shown in Table I. It shows the G2020 has a 17% smaller footprint and is 18% lighter than the predecessor G9000 series [74]. Fig. 18 shows an efficiency plot for the G2020 UPS under different load conditions. This design achieves 98.2% maximum efficiency, the highest in the industry for a double-conversion UPS. The conversion loss is reduced by nearly 50%, delivering 98% efficiency over a wide load range from 30 to 75%. Mitsubishi has also launched its 500 kVA UPS (SUMMIT Series) with similar performance. Series with higher power ratings, such as 750 kVA, are under development as well.

C. Railway Traction Inverter

For railway traction applications, low power loss, light weight, high voltage rating, and high temperature resistance are preferred [75]. Reducing the weight and size of the traction system leaves more space for passengers. Depending on the voltage level and device adopted, a railway traction inverter could be configured as either a three-level or two-level structure. Traditionally, a three-level structure is preferable because of the limited switching frequency capability of Si IGBTs. A two-level traction drive system based on a 3.3 kV/1200 A Si IGBT/SiC JBS diode was developed by Hitachi [76]. It can reduce total losses by 35%, resulting in a 40% reduction in system weight and volume. Mitsubishi has successfully developed a 3.3 kV/1500 A module for all-SiC traction inverters, including a two-level inverter for a 1.5 kV input dc system for the Odakyu Electric Railway and a three-level inverter for 2.5 kV ac input for the central Japan railway [77]. Fig. 19 shows the world's first full-SiC traction system developed for N700 Shinkansen bullet trains on the central Japan railway. Compared with the existing design, it reduces the inverter size by 55% and weight by 35%.

Fig. 19. Mitsubishi all-SiC modules based traction converter [77].

Fig. 20. Toyota SiC power control unit [81].

D. Electric Vehicle

SiC devices are enablers for high power density, which is the most important requirement for power electronics circuits in EVs, almost comparable in importance to cost. The EV Everywhere Challenge announced in 2013 requires a 35% reduction in size and 40% reduction in weight and loss, which can be achieved with a transition to SiC power devices [78]. As the cost of these devices drops, more and more EV manufacturers will be using SiC devices. Toyota has already demonstrated an all-SiC power control unit (PCU) that might be in vehicles by 2020 [79]–[81]. The goal is to reduce the PCU size by 80%. Fig. 20 shows a prototype of a highly compact SiC PCU from Toyota [81]. Ford Motor Company's results in [82] show that switching losses can be reduced by 40% when SiC MOSFETs are used, with an overall 5% improvement in fuel efficiency.

The power electronics circuits in electric drive systems typically include a buck/boost dc–dc converter (currently used only in hybrid EVs) that increases the battery voltage (currently up to 700 V), a traction inverter, a dc–dc converter for auxiliary loads (high-voltage bus to 14 and 42 V conversion), and an onboard charger (OBC).

1) The buck/boost converter requires higher voltage-rated devices (1.2 kV) that can run at high frequencies in the tens of kilohertz, e.g., a 20-kW buck/boost converter running at 100 kHz. The ideal device for this application today would be SiC based. Running at high frequencies allows the filter components to be much smaller, resulting in higher power density. To achieve these high frequencies, power device packages must be designed with minimum parasitic inductance on the order of less than 10 nH. Toyota, in [83], shows a 30% reduction in losses in a boost converter just by replacing the Si PIN diodes with SiC SBD, resulting in a 0.5% efficiency increase for the boost converter.
2) The traction inverter does not need higher switching operation, but lower loss switching and conduction will result in lower losses and less need for thermal management. SiC-based devices rated at 900 and 1200 V are ideal as traction inverter power devices. There is talk about going higher than the current 700 V dc bus voltages for lower losses and higher efficiencies. This would mean that traction motors would be more compact for the same power levels.
3) The dc–dc converter for auxiliary loads has a high-voltage interface and low-voltage interface (14 or 42 V, or both), which require high-voltage and low-voltage devices. The best candidates for the high-voltage side are SiC-based power switches. High-frequency operation of the devices allows the dc–dc converter to be much smaller than the devices available presently.
4) Present-day OBCs are designed for wired operation, but future versions will have wired and wireless options or both. Typical OBCs will require high-frequency switching devices. In [84], Toyota and APEI show a 6 kW SiC OBC system switching at 250 kHz at 95% efficiency with a ten times improvement in power density. In [85], a 6.8 kW SiC-based integrated charger with a 2% improvement in efficiency and 50% reduction in component count was demonstrated.

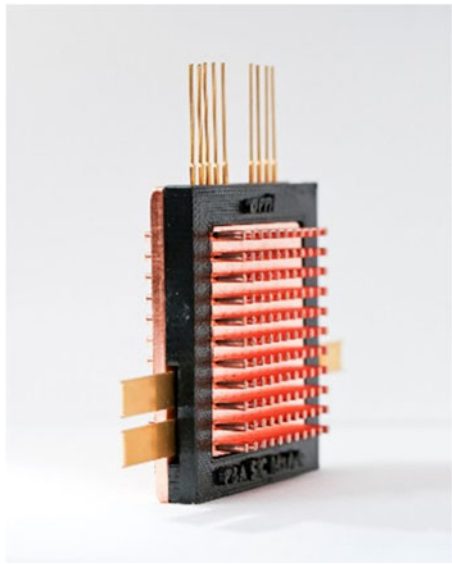

Fig. 21. Double-sided package with pin fin cooling.

Since SiC devices are much smaller than their Si counterparts, it is difficult to reliably package them and cool them as needed. In electric drivetrain technology, the trend is toward double-sided packaging, as shown in Fig. 21, to eliminate wire bonds,

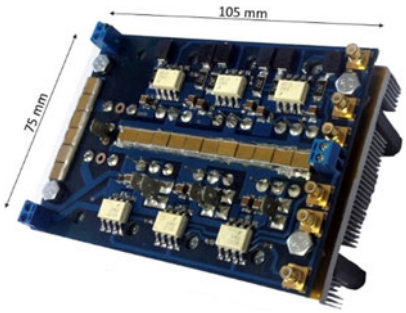

Fig. 22. 6-kW dual-output boost resonant inverter featuring SiC JFET devices for IH applications [90].

Fig. 23. Solid-state transformer based on 15 kV SiC MOSFET [95].

enhance cooling efficiency, and reduce parasitic inductances [86]. The most recent versions of Toyota hybrid EVs [87] and the second-generation Chevy Volt [88] use double-sided packages. The reliability and repeatability issues associated with the manufacturing of double-sided packages are a concern.

E. Induction Heating

IH is a relevant example of a technology that is boosting its performance and application range by using SiC devices [89]. Resonant power converters usually operate at several tens of kilohertz to the megahertz range, and the power range varies from kilowatts in domestic and medical applications to several megawatts in industrial applications. These designs imply challenges regarding blocking voltages, switching losses, and operation in harsh environments that perfectly match the features of SiC devices, opening the design window to high-performance converters and innovative IH applications. Recently, several IH designs taking advantage of WBG devices have been reported, including the use of SiC devices for boost inverters (see Fig. 22) [90], ac−ac converters [91], and dual-frequency IH systems [92]. Different technologies, including BJTs, JFETs, and MOSFETs, are compared in [93], proving the potential benefits for IH applications. Future challenges for IH systems include the design of reliable systems with increased ratings in terms of voltage and current for SiC devices.

F. High-Voltage SiC Device Applications

High-voltage SiC devices provide significantly higher voltage–frequency capability, which enables medium-voltage and high-frequency power conversion. One such application is the solid state transformer [9], [50], [94]. Fig. 23 shows a 1 MVA solid state transformer based on a 15 kV/120 A SiC MOSFET module. Compared with a traditional transformer with the same rating, it facilitates a 50% reduction in size and 75% reduction in weight while achieving 98% efficiency. Another potential application of high-voltage SiC devices is the circuit breaker. The SiC ETO has been applied to both circuit breakers and hybrid circuit breakers for the medium-voltage grid [64]. In addition, a high-voltage SiC power electronics building block (PEBB) concept is being investigated for general-purpose medium- to high-voltage applications [49].

IV. Challenges and Trends

Although SiC devices show promising advantages, many challenges exist from both the device and application perspectives. These guide future research and development trends.

1) The field reliability of SiC devices must be demonstrated for various applications, and a voltage-derating design guideline needs to be established. This is especially important for applications in which reliability is extremely critical, such as aviation systems [45]. On the one hand, a power conversion system with SiC device potentially provides a higher current rating than one with a Si device, which leads to a larger thermal ripple. On the other hand, the higher temperature operation of the SiC device indicates more stringent requirement for the package materials.
2) Manufacturing processes need to be improved for better yields to make the costs of SiC devices more justifiable for system applications [44]. Most major SiC manufacturers are making a transition to 150 mm SiC epitaxial wafers. In addition, there are discussions about going to a fabless manufacturing process, in which SiC power devices can be manufactured in Si fabs. Such a move would lower costs, because the existing facilities and mature manufacturing infrastructure would guarantee the quality. However, the lack of flexibility in processes and SiC tools is challenging.
3) SiC devices switch much faster than Si devices, which poses challenges to the gate driver design [95], [96]. First, the higher dv/dt of the SiC device injects a higher common mode current to the gate loop through a miller capacitor and thus induces a positive spurious gate voltage. An advanced gate driver with active dv/dt and di/dt control is a trend. Additionally, the higher dv/dt injects a higher common mode current to the primary side of the gate driver through the isolation barrier, which sets the limits of the coupling capacitance. Second, SiC devices have a faster current rise during the fault condition in addition to a smaller die size. Therefore, the short circuit protection response requirement of the gate driver is higher. Finally, the parallel or series connection of the SiC device is also more sensitive to the timing mismatch.

4) The innovative EMI filter design needs to be investigated [97]. The faster switching transient combined with a higher switching frequency contributes to EMI noise that is from 10 to 100 times higher. This becomes especially challenging for high-voltage and high-power applications. On the one hand, the modeling and prediction methodology of EMI noise for SiC power converters is indispensable. On the other hand, innovative shielding techniques and filter designs are needed.
5) Novel system layouts with a minimized commutation loop are critical, including both the SiC device package and system busbar layout [71]. Although it is acknowledged that a SiC power converter can deliver higher current, this statement is true only when the device voltage stress during the transition is less than its breakdown voltage. In other words, the current rating of the system may be limited by the voltage overshoot instead of the thermal. For some emerging applications, such as the 1.5 kV DC photovoltaic system, this issue is critically important. Laminated and multilayer laminated busbar structures are the solution of choice so far. In addition, a low-inductance capacitor needs to be investigated.
6) The smaller die size of SiC chips and the corresponding higher loss density open new design challenges for thermal management strategies [86]. In addition, the smaller thermal capacitance of the SiC chips may result in higher temperature ripple, raising challenge from the reliability perspective. Some efficient cooling methods—such as double-sided cooling, liquid jet impingement cooling, and phase change cooling—are potential promising solutions [98]. Furthermore, the emerging three-dimensional (3-D)-printed technologies can be potentially used to enable creative solutions.
7) The high-temperature operation capability of SiC power devices requires innovations in peripheral components, such as high-temperature capacitors, packages, control electronics, gate drivers, and sensors [99]. Capacitors are particularly challenging, since the bus bars connecting the high-temperature devices to the capacitors further increase the capacitor temperature. Cooling of the capacitors might be needed to enable their use with high-temperature switches. In addition, high-temperature-rated gate drivers based on Si-on-insulator (SOI) or SiC are needed. SOI technology is typically limited to 225 °C or lower. SiC-based integrated circuit design is challenging since the SiC has a lower channel mobility, which makes it not suitable for very low-voltage applications.
8) For many potential SiC users, the high nonrecurring engineering cost is also a concern because of limited knowledge of these new devices. Similar to the Si PEBB, the standard SiC PEBB can significantly reduce engineering effort and development costs, paving the way for commercialization of SiC applications [100]. The low-inductance busbar, high-bandwidth and noise-free controller, and robust gate driver, as well as the heat sink, could be integrated. The whole system could then be built directly around this PEBB for various applications.

V. Conclusion

SiC devices and power electronics systems have received tremendous attention from both academia and industry in the past decade. This paper presented a systematic review of major emerging SiC technologies applications. In addition, the design challenges and future development trends are summarized. It is evident that the performance SiC devices have improved significantly and SiC power conversion systems are being accepted by industry and demonstrated in many critical applications such as solar, traction, UPS, and EVs. It can be concluded that SiC will revolutionize the whole energy conversion industry.

References

[1] J. G. Kassakian and T. M. Johns, "Evolving and emerging applications of power electronics in systems," *IEEE J. Emerg. Sel. Topics Power Electron.*, vol. 1, no. 2, pp. 47–58, Jun. 2013.
[2] J. D. Van Wyk and F. C. Lee, "On a future for power electronics," *IEEE J. Emerg. Sel. Topics Power Electron.*, vol. 1, no. 2, pp. 59–72, Jun. 2013.
[3] J. Millan, P. Godignon, X. Perpina, A. P. Tomas, and J. Rebollo, "A survey of wide bandgap power semiconductor devices," *IEEE Trans. Power Electron.*, vol. 29, no. 5, pp. 2155–2163, May 2014.
[4] P. Roussel, "SiC market and industry update," presented at the Int. SiC Power Electron. Appl. Workshop, Kista, Sweden, 2011.
[5] J. W. Palmour, "Silicon carbide power device development for industrial markets," in *Proc. IEEE IEDM.*, 2014, pp. 1.1.1–1.1.8.
[6] *The World Market for Silicon Carbide and Gallium Nitride Power Semiconductors—2013 Edition*, vol. 9790. Wellingborough, U.K.: HIS, 2013.
[7] K. Madjour, "Silicon carbide market update: From discrete devices to modules," presented at the PCIM Europe, Nuremberg, Germany, 2014 .
[8] F. Dahlquist, "Junction barrier Schottky rectifiers in silicon carbide," Ph.D. dissertation, Dept. Microelectron. Inf. Technol., Royal Inst. Technol., Brinellvägen, Sweden, 2002.
[9] F. Wang, G. Wang, A. Q. Huang, W. Yu, and X. Ni, "Design and operation of a 3.6 kV high performance solid state transformer based on 13 kV SiC MOSFET and JBS diode," in *Proc. IEEE ECCE*, 2014, pp. 4553–4560.
[10] O. Harmon, T. Basler, and F. Bjork. (2015, Dec.). *Advantages of the 1200 V SiC Schottky Diode with MPS Design* pp. 34–37. [Online]. Available: www.bodospower.com
[11] L. D. Benedetto, G. D. Licciardo, T. Erlbacher, A. J. Bauer, and S. Bellone, "Analytical model and design of 4H-SiC planar and trench JBS diode," *IEEE Trans. Electron. Devices.*, vol. 63, no. 6, pp. 2474–2481, Jun. 2016.
[12] C. Bodeker, T. Vogt, and N. Kaminski, "Stability of SiC Schottky diode against leakage current thermal runaway," in *Proc. Int. Symp. Power Semicond. Devices ICs*, 2015, pp. 245–248.
[13] T. Kimoto, "Ultrahigh-voltage SiC devices for future power infrastructure," in *Proc. ESSDERC*, Sep. 2013, pp. 22–29.
[14] R. Singh *et al.*, "Large area, ultra-high voltage 4H-SiC p-i-n rectifiers," *IEEE Trans. Electron. Device*, vol. 49, no. 12, pp. 2308–2316, Dec. 2002.
[15] X. Wang and J. A. Cooper, Jr., "Optimization of JTE edge terminations for 10 kV power devices in 4H SiC," *Mater. Sci. Forum*, vol. 457–460, pp. 1257–1260, 2003.
[16] D. C. Sheridan, G. Niu, and J. D. Cressler, "Design of single and multiple zone junction termination extension structures for SiC power devices," *Solid State Electron.*, vol. 45, pp. 1659–1664, 2001.
[17] M. K. Dasa, B. A. Hull, J. T. Richmond, B. Heath, J. J. Sumakeris, and A. R. Powell, "Ultra high power 10 kV, 50 A SiC PiN diodes," in *Proc. Int. Symp. Power Semicond. devices ICs*, 2005, pp. 299–302.
[18] H. Onose, S. Oikawa, T. Yatsuo, and Y. Kobayashi, "Over 2000 V FLR termination technologies for SiC high voltage devices," in *Proc. Int. Symp. Power Semicond. devices ICs*, 2000, pp. 245–248.
[19] D. C. Sheridan, G. Niu, J. N. Merrett, J. D. Cressler, C. Ellis, and C. C. Tin, "Design and fabrication of planar guard ring termination for high-voltage SiC diodes," *Solid State Electron.*, vol. 44, no. 8, pp. 1367–1372, Aug. 2000.
[20] V. Saxena, J. N. Su, and A. J. Steckl, "High voltage Ni- and Pt-SiC Schottky diodes using metal field plate edge termination," *IEEE Trans. Electron Devices*, vol. 46, no. 3, pp. 456–464, Mar. 1999.

[21] M. C. Tarplee, V. P. Madangarli, Q. Zhang, and S. Sudardhan, "Design rules for field plate edge termination in SiC Schottky diodes," *IEEE Trans. Electron. Devices*, vol. 48, no. 12, pp. 2659–2664, Dec. 2001.

[22] T. Hiyoshi, T. Hori, J. Suda, and T. Kimoto, "Simulation and experimental study on the junction termination structures for high voltage 4H-SiC pin diodes," *IEEE Trans. Electron Devices*, vol. 55, no. 8, pp. 1841–1846, Aug. 2008.

[23] S. Sundaresan, M. Marripelly, S. Arshavsky, and R. Singh, "15 kV SiC PiN diodes achieve 95% of avalanche limit and stable long-term operation," in *Proc. Int. Symp. Power Semicond. Devices ICs*, 2013, pp. 175–177.

[24] W. Sung, J. Baliga, and A. Q. Huang, "Area-efficient bevel-edge termination techniques for SiC high-voltage devices," *IEEE Trans. Electron. Devices*, vol. 63, no. 4, pp. 1630–1636, Apr. 2016.

[25] X. Li, K. Tone, L. H. Cao, P. Alexandrov, L. Fursin, and J. H. Zhao, "Theoretical and experimental study of 4H-SiC junction edge termination," *Mater. Sci. Forum*, vol. 338−342, pp. 1375–1379, 2000.

[26] R. Perez, D. Tournier, A. Perez-Tomas, P. Godignon, N. Mestres, and J. Millan, "Planar edge termination design and technology considerations for 1.7 kV 4H-SiC pin diodes," *IEEE Trans. Electron. Devices*, vol. 52, no. 10, pp. 2309–2316, Oct. 2005.

[27] Y. Sugawara, D. Takayama, K. Asano, R. Singh, J. Palmour, and T. Hayashi, "12–19 kV 4H-SiC PiN diodes with low power loss," in *Proc. Int. Symp. Power Semicond. Devices ICs*, 2001, pp. 27–30.

[28] K. Kinoshita, T. Hatakeyama, O. Takikawa, A. Yahata, and T. Shinohe, "Guard ring assisted RESURF: A new termination structure providing stable and high breakdown voltages for SiC power devices," in *Proc. Int. Symp. Power Semicond. Devices ICs*, 2002, pp. 253–256.

[29] W. Sung, "Design and fabrication of 4H-SiC high voltage devices," Ph.D. dissertation, Dept. Elect. Comput. Eng., North Carolina State Univ., Raleigh, NC, USA, 2011.

[30] P. A. Losee, S. Balachandran, L. Zhu, T. P. Chow, I. Bhat, and R. J. Gutmann, "High voltage 4H-SiC pin rectifiers with single-implant, multi-zone JTE termination," in *Proc. Int. Symp. Power Semicond. Devices ICs*, 2004, pp. 301–304.

[31] W. Sung, E. Van Brunt, B. J. Baliga, and A. Q. Huang, "A new edge termination technique for high-voltage devices in 4H-SiC—Multiple-floating-zone junction termination extension," *IEEE Electron. Device Lett.*, vol. 32, no. 7, pp. 880–882; July. 2011.

[32] G. Feng, J. Suda, and T. Kimoto, "Space-modulated junction termination extension for ultrahigh-voltage PiN diodes in 4H-SiC," *IEEE Trans. Electron Devices*, vol. 59, no. 2, pp. 414–418, Feb. 2012.

[33] H. Niwa, G. Feng, J. Suda, and T. Kimoto, "Breakdown characteristics of 15-kV-class 4H-SiC PiN diodes with various junction termination structures," *IEEE Trans. Electron. Devices*, vol. 59, no. 10, pp. 2748–2752, Oct. 2012.

[34] S. Guo *et al.*, "3.38 MHz operation of 1.2 kV SiC MOSFET with integrated ultra-fast gate drive," in *Proc. IEEE Third Workshop Wide Bandgap Power Devices Appl.*, pp. 390–395, 2015.

[35] L. Cheng and J. W. Palmour, "Cree's SiC power MOSFET technology: Present status and future perspective," presented at the Ninth Annual SiC MOS Workshop, 2014.

[36] P. Losee *et al.*, "1.2 kV class SiC MOSFETs with improved performance over wide operating temperature," in *Proc. Int. Symp. Power Semicond. Devices ICs*, 2014, pp. 297–300.

[37] C. M. Dimarino, R. Burgos, and D. Boroyevich, "High-temperature silicon carbide: Characterization of state-of-art silicon carbide power transistors," *IEEE Ind. Electron. Mag.*, vol. 9, no. 3, pp. 19–30, Sep. 2015.

[38] T. Nakamura *et al.*, "High performance SiC trench devices with ultra-low Ron," in *Proc. IEEE IEDM*, 2011, pp. 26.5.1–26.5.3.

[39] 1200 V/180 A Full SiC Power Module with Integrated SiC Trench MOSFET, 2016. [Online]. Available: www.rohm.co.jp

[40] X. Song, A. Q. Huang, M. Lee, and C. Peng, "High voltage Si/SiC hybrid switch: An ideal next step for SiC," in *Proc. Int. Symp. Power Semicond. Devices ICs*, 2015, pp. 289–292.

[41] M. Rahimo *et al.*, "Characterization of a Si IGBT and silicon carbide MOSFET cross-switch hybrid," *IEEE Trans. Power Electron.*, vol. 30, no. 9, pp. 4638–4642, 2016.

[42] D. Heer, D. Domes, and D. Peters, "Switching performance of a 1200 V SiC-trench-MOSFET in a low-power module," in *Proc. PCIM Europe*, 2016, pp. 53–59.

[43] J. Lutz and R. De Doncker, *Semiconductor Power Devices: Physics, Characteristics, and Reliability*. Springer, 2011.

[44] J. Casady, "Power products commercial roadmap for SiC from 2012–2020," in *Proc. US DOE High MW Direct-Drive Motor Workshop*, 2014.

[45] A. Bolotnikov *et al.*, "Overview of 1.2 kV–2.2 kV SiC MOSFETs targeted for industrial power conversion applications," in *Proc. IEEE APEC*, 2015, pp. 2445–2452.

[46] A. Bolotnikov *et al.*, "3.3 kV SiC MOSFETs designed for low on-resistance and fast switching," in *Proc. Int. Symp. Power Semicond. Devices ICs*, 2012, pp. 389–392.

[47] V. Pala *et al.*, "10 kV and 15 kV silicon carbide power MOSFETs for next-generation energy conversion and transmission systems," in *Proc. IEEE ECCE*, 2014, pp. 449–454.

[48] J. B. Casady *et al.*, "New generation 10 kV SiC power MOSFET and diodes for industrial applications," in *Proc. PCIM Europe*, 2015, pp. 1–8.

[49] C. DiMarino, I. Cvetkovic, Z. Shen, R. Burgos, and D. Boroyevich, "10 kV, 120 A SiC MOSFET modules for a power electronics building block (PEBB)," in *Proc. IEEE WiPDA*, 2014, pp. 55–58.

[50] X. She, A. Q. Huang, and R. Burgos, "Review of solid-state transformer technologies and their application in power distribution systems," *IEEE J. Emerg. Sel. Topics Power Electron.*, vol. 1, no. 3, pp. 186–198, Sept. 2013.

[51] M. K. Das *et al.*, "State of the art 10 kV NMOS transistors," in *Proc. Int. Symp. Power Semicond. Devices ICs*, 2008, pp. 253–255.

[52] M. K. Das *et al.*, "A 13 kV 4H-SiC n-channel IGBT with low Rdiff, on and fast switching," *Mater. Sci. Forum*, vol. 600–603, pp. 1183–1186, 2009.

[53] X. Wang and J. A. Cooper, "High-voltage N-channel IGBTs on free-standing 4H-SiC epilayers," *IEEE Trans. Electron. Devices*, vol. 57, no. 2, pp. 511–515, Feb. 2010.

[54] S. Ryu *et al.*, "Ultra high voltage (>12 kV), high performance 4H-SiC IGBTs," in *Proc. Int. Symp. Power Semicond. Devices ICs*, 2012, pp. 257–260.

[55] S. Ryu *et al.*, "Ultra high voltage IGBTs in 4H-SiC," in *Proc. IEEE WiPDA*, 2013, pp. 36–39.

[56] E. Van Brunt *et al.*, "22 kV, 1 cm^2, 4H-SiC n-IGBTs with improved conductivity modulation," in *Proc. Int. Symp. Power Semicond. Devices ICs*, 2014, pp. 358–361.

[57] E. Van Brunt *et al.*, "27 kV, 20 A 4H-SiC n-IGBTs," *Mater. Sci. Forum*, vol. 821–823, pp. 847–850, 2015.

[58] K. Fukuda *et al.*, "Development of ultra high voltage SiC power devices," *IEEE Trans. Electron. Devices*, vol. 62, no. 2, pp. 396–404, Feb. 2015.

[59] Q. Zhang *et al.*, "10 kV trench gate IGBTs on 4H-SiC," in *Proc. Int. Symp. Power Semicond. Devices ICs*, 2005, pp. 303–306.

[60] Q. Zhang, C. Jonas, S. Ryu, A. Agarwal, and J. Palmour, "New improvement results on 7.5 kV 4H-SiC p-IGBTs with Rdiff, of 26 mΩ·cm2 at 25 °C," in *Proc. Int. Symp. Power Semicond. Devices ICs*, 2007, pp. 281–284.

[61] Q. Zhang, C. Jonas, J. Sumakeris, A. Agarwal, and J. Palmour, "12 kV 4H-SiC p-IGBTs with record low specific on-resistance," in *Proc. Int. Conf. Silicon Carbide Related Mater.*, Otsu, Japan, Oct. 14–19, 2007.

[62] Q. Zhang *et al.*, "Design and characterization of high-voltage 4H-SiC p-IGBTs," *IEEE Trans. Electron. Devices*, vol. 55, no. 8, pp. 1912–1919, Aug. 2008.

[63] L. Cheng *et al.*, "Advanced silicon carbide gate turn-off thyristor for energy conversion and power grid applications," in *Proc. IEEE ECCE*, 2012, pp. 2249–2252.

[64] A. Q. Huang, C. Peng, and X. Song, "Design and development of a 7.2 kV/200 A hybrid circuit breaker based on 15 kV SiC emitter turn-off (ETO) thyristor," in *Proc. IEEE ESTS*, 2015, pp. 306–311.

[65] U. Schwarzer, S. Buschhorn, and K. Vogel, "System benefits for solar inverters using SiC semiconductor modules," in *Proc. PCIM Europe*, 2014, pp. 787–794.

[66] S. Buschhorn and K. Vogel, "Saving money: SiC in UPS applications," in *Proc. PCIM Europe*, 2014, pp. 765–771.

[67] A. Vergara, N. Henze, N. Engler, and P. Zacharias, "A single-stage PV module integrated converter based on a low power current-source inverter," *IEEE Trans. Ind. Electron.*, vol. 55, no. 7, pp. 2602–2609, Jul. 2008.

[68] B. Chen, B. Gu, L. Zhang, and J. Lai, "A novel pulse-width modulation method for reactive power generation on a CoolMOS- and SiC-diode-based transformerless inverter," *IEEE Trans. Ind. Electron.*, vol. 63, no. 3, pp. 1539–1548, Mar. 2016.

[69] J. Mookken, B. Agrawal, and J. Liu, "Efficient and compact 50 kW Gen2 SiC device based PV string inverter," in *Proc. PCIM Europe*, 2014, pp. 780–786.

[70] K. Fujii, Y. Noto, M. Oshima, and Y. Okuma, "1-MW solar power inverter with boost converter using all SiC power module," in *Proc. ECCE Europe*, 2015, pp. 1–10.
[71] M. H. Todorovic *et al.*, "SiC MW solar inverter," in *Proc. PCIM Europe*, 2016, pp. 645–652.
[72] J. McBryde, A. Kadavelugu, B. Compton, S. Bhattacharya, M. Das, and A. Agarwal, "Performance comparison of 1200 V silicon and SiC devices for UPS application," in *Proc. IEEE IECON*, 2010, pp. 2657–2662.
[73] N. Epp, C. S. Overbeck, Z. Cao, M. Lemke, and L. Heinemann, "SiC improves switching losses, power density and volume in UPS," in *Proc. PCIM Europe*, 2016, pp. 1677–1684.
[74] G2020 Series SiC 500–750 kVA, (2016). [Online]. Available: http://www.toshiba.com /tic/power-electronics/uninterruptible-power-systems /g2020-series-sic-500-to-750-kva
[75] P. Ladoux, M. Mermet, J. Casarin, and J. Fabre, "Outlook for SiC devices in traction converters," in *Proc. Elect. Syst. Aircraft, Railway Ship Propulsion*, 2012, pp. 1–6.
[76] K. Ishikawa, K. Ogawa, S. Yukutake, and N. Kameshiro, "Traction inverter that applies compact 3.3 kV/1200 A SiC hybrid module," in *Proc. Int. Power Electron. Conf.*, 2014, pp. 2140–2144.
[77] Products: Transportation Systems, (2016). [Online]. Available: http://www.MitsubishiElectric.com/products/transportation/
[78] US DOE EV Everywhere Grand Challenge Blueprint. (2013, Jan. 31). [Online]. Available: http://energy.gov/sites/prod/files/2014/02/f8/eveverywhere_blueprint.pdf
[79] K. Hamada, M. Nagao, M. Ajioka, and F. Kawai, "SiC-emerging power device technology for next-generation electrically powered environmentally friendly vehicles," *IEEE Trans. Electron. Devices*, vol. 62, no. 2, pp. 278–285, Feb. 2015.
[80] T. Ogawa, A. Tanida, T. Yamakawa, and M. Okamura, "Verification of fuel efficiency improvement by application of highly effective silicon carbide power semiconductor to HV inverter," SAE Tech. Paper 2016-01-1230, 2016, doi: 10.4271/2016- 01-1230.
[81] Toyota to Trial New SiC Power Semiconductor Technology. (2015, Jan. 29). [Online]. Available: http://newsroom.toyota.co.jp/en/detail/5692153.
[82] M. Su, C. Chen, S. Sharma, and J. Kikuchi, "Performance and cost considerations for SiC-based HEV traction inverter systems," in *Proc. IEEE Third Workshop Wide Bandgap Power Devices Appl.*, pp. 347–350, 2015.
[83] T. Sugiura, A. Tanida, and K. Tamura, "Efficiency improvement of boost converter for fuel cell bus by silicon carbide diodes," *SAE Int. J. Alt. Power*, vol. 5, no. 2, 2016, doi: 10.4271/2016-01-1234.
[84] K. Shiozaki, K. Toshiyuki, J. Lee, and K. Miyagi, "Verification of high frequency SiC on-board vehicle battery charger for PHV," SAE Tech. Paper 2016-01-1210, 2016, doi: 10.4271/2016-01-1210.
[85] G.-J. Su and L. Tang, "An integrated onboard charger and accessory power converter using WBG devices," in *Proc. IEEE Energy Convers. Congr. Expo.*, 2015, pp. 6306–6313.
[86] P. Ning, Z. Liang, and F. Wang, "Double-sided cooling design for novel planar module," in *Proc. IEEE Appl. Power Electron. Conf.*, 2013, pp. 616–621.
[87] O. Kitazawa, T. Kikuchi, M. Nakashima, and Y. Tomita, "Development of power control unit for compact-class vehicle," *SAE Int. J. Alt. Power*, vol. 5, no. 2, 2016, doi: 10.4271/2016-01-1227.
[88] M. Anwar, M. Hayes, A. Tata, and M. Teimorzadeh, "Power dense and robust traction power inverter for the second generation Chevrolet Volt extended-range EV," *SAE Int. J. Alt. Power*, vol. 4, no. 1, 2015, doi: 10.4271/2015-01-1201.
[89] O. Lucia, P. Maussion, E. J. Dede, and J. M. Burdio, "Induction heating technology and its applications: Past developments, current technology, and future challenges," *IEEE Trans. Ind. Electron.*, vol. 61, no. 5, pp. 2509–2520, May 2014.
[90] H. Sarnago, O. Lucia, A. Mediano, and J. M. Burdio, "Design and implementation of a high-efficiency multiple-output resonant converter for induction heating applications featuring wide bandgap devices," *IEEE Trans. Power Electron.*, vol. 29, no. 5, pp. 2539–2549, 2014.
[91] T. Mishima, S. Morinaga, and M. Nakaoka, "All-SiC power module-applied single-stage ZVS-PWM AC−AC converter for high-frequency induction heating," in *Proc. IEEE IECON*, 2015, pp. 004211–004216.
[92] V. Esteve *et al.*, "Comparative study of a single inverter bridge for dual-frequency induction heating using Si and SiC MOSFETs," *IEEE Trans. Ind. Electron.*, vol. 62, no. 3, pp. 1440–1450, Mar. 2015.
[93] H. Sarnago, O. Lucia, and J. M. Burdio, "A comparative evaluation of SiC power devices for high-performance domestic induction heating," *IEEE Trans. Ind. Electron.*, vol. 62, no. 8, pp. 4795–4804, 2015.
[94] M. K. Das, C. Capell, D. E. Grider, R. Raju, M. Schutten, and J. Nasadosk, "10 kV, 120 A SiC half-bridge power MOSFET modules suitable for high frequency, medium voltage applications," in *Proc. IEEE ECCE*, 2011, pp. 2689–2692.
[95] D. P. Sadik *et al.*, "Short-circuit protection circuits for silicon-carbide power transistors," *IEEE Trans. Ind. Electron.*, vol. 63, no. 4, pp. 1995–2004, Apr. 2016.
[96] J. Hu *et al.*, "Robustness and balancing of parallel-connected power devices: SiC versus CollMOS," *IEEE Trans. Ind. Electron.*, vol. 63, no. 4, pp. 2092–2102, Apr. 2016.
[97] X. Gong and J. A. Ferreira, "Investigation of conducted EMI in SiC JFET inverters using separated heat sinks," *IEEE Trans. Ind. Electron.*, vol. 61, no. 1, pp. 115–125, Jan. 2014.
[98] E. Laloya, O. Lucia, H. Sarnago, and J. M. Burdio, "Heat management in power converters: From state of the art to future ultrahigh efficiency systems," *IEEE Trans. Power Electron.*, vol. 31, no. 11, pp. 7896–7908, Nov. 2016.
[99] P. Ning *et al.*, "High temperature hardware: Development of a 10-kw high-temperature, high-power density three phase ac—dc–ac SiC converter," *IEEE Ind. Electron. Mag.*, vol. 7, no. 1, pp. 6–17, Mar. 2013.
[100] X. She *et al.*, "High performance SiC power block for industry applications," in *Proc. IEEE ECCE*, 2016, pp. 1–4.

Xu She (S'08−M'13−SM'15) received the B.Sc. and M.Sc. degrees from Huazhong University of Science and Technology, Huazhong, China, in 2007 and 2009, respectively, and the Ph.D. degree from North Carolina State University, Raleigh, NC, USA, in 2013.

His Ph.D. work on solid-state transformers was named and cited by *MIT Review* as one of the top ten emerging technologies in 2011. He is currently a Lead Electrical Engineer in the Power Electronics Laboratory, GE Global Research Center, Niskayuna, NY, USA. His current research interests include high-power-density, high-efficiency, and high-frequency power conversion systems, in particular, SiC power conversion systems and solid-state transformers. He has authored or coauthored over 55 papers published in the refereed journals and international conference proceedings and has more than 20 patents issued/filed.

Dr. She received the Chinese Government Award of Outstanding Graduate Student Abroad in 2013. He has received one IEEE Best Paper Award.

Alex Q. Huang (S'91−M'94−SM'96−F'05) received the B.Sc. degree from Zheijiang University, Zheijiang, China, in 1983, the M.Sc. degree from Chengdu Institute of Radio Engineering, Chengdu, China, in 1986, and the Ph.D. degree from Cambridge University, Cambridge, U.K., in 1992.

From 1994 to 2004, he was a Professor at the Center for Power Electronics Systems, Virginia Polytechnic Institute and State University. Since 2004, he has been with North Carolina State University, Raleigh, NC, USA, where he is currently the Progress Energy Distinguished Professor of Electrical and Computer Engineering. He established the NSF FREEDM Systems ERC in 2008. His current research interests include power electronics, power management microsystems, and power semiconductor devices. He has mentored more than 70 Ph.D. and Master's students and has published more than 450 papers and has been granted more than 20 U.S. patents.

Prof. Huang is the recipient of an NSF CAREER Award, the prestigious R&D 100 Award, and the *MIT Technology Review* 2011 Technology of the Year Award.

Óscar Lucía (S'04–M'11–SM'14) received the M.Sc. and Ph.D. degrees (with honors) in electrical engineering from the University of Zaragoza, Zaragoza, Spain, in 2006 and 2010, respectively.

Since 2008, he has been with the Department of Electronic Engineering and Communications, University of Zaragoza, where he is currently an Associate Professor. His current research interests include resonant power conversion, wide-bandgap devices, and digital control, mainly applied to contactless energy transfer, induction heating, and biomedical applications. On these topics, he has published more than 50 international journal papers and 100 conference papers. He has filed more than 25 patents.

Dr. Lucía is an Associate Editor of the IEEE TRANSACTIONS ON INDUSTRIAL ELECTRONICS and the IEEE TRANSACTIONS ON POWER ELECTRONICS. He is a member of the Aragon Institute for Engineering Research (I3A).

Burak Ozpineci (S'92–M'02–SM'05) received the B.S. degree in electrical engineering from Orta Dogu Technical University, Ankara, Turkey, in 1994, and the M.S. and Ph.D. degrees in electrical engineering from The University of Tennessee, Knoxville, TN, USA, in 1998 and 2002, respectively.

He joined the Post-Masters Program with the Power Electronics and Electric Machinery (PEEM) Group, Oak Ridge National Laboratory (ORNL), Knoxville, TN, USA, in 2001, and became a Full-Time Research and Development Staff Member in 2002 and Group Leader of the Power and Energy Systems Group in 2008. He is currently leading the PEEM and managing the Electric Drive Technologies Program at ORNL. He also serves as a Joint Faculty Associate Professor with The Bredesen Center, The University of Tennessee, Knoxville. His current research interests include system-level impact of wide bandgap power devices, power electronics for electric and hybrid electric vehicles, advanced manufacturing of power electronics, and wireless power transfer.